pH > 4

pH < 4

Themed issue: Self-organisation of nanoparticles

PAPER
Jorge Pérez-Juste *et al.*
Reversible assembly of metal nanoparticles induced by penicillamine. Dynamic formation of SERS hot spots

Reversible assembly of metal nanoparticles induced by penicillamine. Dynamic formation of SERS hot spots†

Patricia Taladriz-Blanco,[a] Niklaas J. Buurma,[b] Laura Rodríguez-Lorenzo,[a] Jorge Pérez-Juste,*[a] Luis M. Liz-Marzán[a] and Pablo Hervés*[a]

We report a systematic study of the surface modification of gold and silver nanoparticles with DL-penicillamine (PEN) and *N*-acetyl-DL-penicillamine (NAP), motivated by the possibility of inducing pH-controlled reversible nanoparticle assembly. The interaction of PEN and NAP with the metal nanoparticle surface was studied by isothermal titration calorimetry (ITC). The results indicate that equilibrium is reached with the formation of a submonolayer corresponding to *ca.* 40% and 64% of total surface coverage for PEN and NAP, respectively. Both PEN and NAP modified nanoparticles could be reversibly aggregated at acidic pH due to the protonation of the carboxylic groups, leading to a decrease in their stability by electrostatic interactions and the advent of hydrogen bonding interactions which promote interparticle linkage. The process was monitored by UV-Vis spectroscopy, transmission electron microscopy (TEM) and surface enhanced Raman scattering (SERS) spectroscopy. Interestingly, the SERS characterization demonstrated the pH-controlled formation of hot-spots.

Introduction

Different methods and tools have been proposed to direct the assembly of nanoparticles, among which Chemistry is considered one of the most relevant ingredients in the toolbox.[1–3] Particularly developed is the modification of the nanoparticles surface chemistry through adsorption of pre-designed molecules that are capable of responding toward different stimuli, leading to the reversible assembly of the particles. Among the different stimuli that have been investigated we can point out temperature,[4] electromagnetic radiation,[5] pH,[6] metal ions,[7] or redox activity,[8] among others. The modulation of such parameters triggers the interaction between the different capping agents and ultimately the extension of the assembly.[9] Typically, these interactions are related to hydrophobic interactions, hydrogen bonding, molecular dipolar interaction, π–π interactions, *etc.* Most of the systems on which chemistry-directed self-assembly has been studied involve gold or silver nanoparticles, which are typically synthesized and subsequently modified with a thiol-containing molecule that is sensitive toward a specific external stimulus. Therefore, the distribution and stoichiometry, *i.e.* the number of capping molecules per particle unit surface (nm²) is highly

relevant. Usually a large excess of capping molecules is added and non-adsorbed molecules are subsequently removed by either centrifugation or dialysis, but in any case the average number of molecules per nanoparticle is difficult to estimate. Indirect methods have been proposed to estimate the number of functional groups at the gold nanoparticle surface allowing further bioconjugation. For example, Maus *et al.* recently presented a fluorescence-based assay for the characterization of functionalized gold nanoparticles capped with a self-assembled monolayer of mixed thiols derived from poly(ethylene glycol) (PEG). The gold nanoparticles carry primary amino groups at the solvent-exposed interface and the reported assay allows quantification of the average number of amino groups that are available for functionalization.[10,11]

Isothermal titration calorimetry (ITC) is a sensitive technique that is routinely used to quantify the thermodynamics of reversible interactions in biological systems.[12] ITC proved successful in studies related to protein–protein interactions,[12,13] protein–DNA interactions,[13,14] protein–lipid interactions,[15] functionalised nanoparticle–protein interactions,[16] *etc.* This technique has also been applied to study the interactions between nanoparticles and different molecules likely to be adsorbed or to react with the nanoparticle surface. For example, Linse *et al.* studied the thermodynamics of binding of human serum albumin (HSA) to copolymer nanoparticles in the size range of 70–700 nm, with different degrees of hydrophobicity.[17] Sastry *et al.* analysed the energetics of interaction of different DNA bases and peptide nucleic acid (PNA) nucleobases with gold nanoparticles,[18] as well as the interactions of several amino acids with

[a]Departamento de Química Física and Unidad Asociada CSIC-Universidade de Vigo, 36310 Vigo, Spain. E-mail: juste@uvigo.es; jherves@uvigo.es; Fax: +34 986812556

[b]Physical Organic Chemistry Centre, School of Chemistry, Cardiff University, Main Building, Park Place, Cardiff, CF10 3AT, UK

† Electronic supplementary information (ESI) available. See DOI: 10.1039/c1jm12175h

gold nanoparticles,[19] while Rao *et al.* studied the interactions between Au NPs and cysteine and mercaptopropionic acid.[20]

In this work, we carried out a systematic study of the interaction of DL-penicillamine (PEN) and its amine protected counterpart *N*-acetyl-DL-penicillamine (NAP), with citrate stabilized metal nanoparticles. The number of available sites at the nanoparticle surface was expected to depend on the size of the binding molecule. To quantify PEN and NAP binding, and therefore the surface coverage, we titrated the amino acid into nanoparticle solutions and monitored the heat response using ITC. The successful surface modification should allow the assembly and disassembly of the nanoparticles by controlling the pH of the dispersions.[6] The pH effect on the reversible assembly–disassembly was characterized in terms of the (plasmon related) optical response, as well as the SERS enhancing capabilities of the aggregates (through plasmon coupling and dynamic hot spot formation).

Experimental section

Chemicals

Tetrachloroauric acid ($HAuCl_4 \cdot 3H_2O$), silver perchlorate ($AgClO_4$) anhydrous (97%), sodium borohydride ($NaBH_4$), and sodium hydroxide were purchased from Aldrich and DL-penicillamine from Fluka. Sodium citrate ($C_6H_5O_7Na_3$) was supplied by Sigma, hydrochloric acid by Panreac and *N*-acetyl-DL-penicillamine hemihydrate (98%) by Alfa Aesar. Milli-Q-grade water was used in all preparations.

Experimental techniques

A JEOL JEM 1010 transmission electron microscope (TEM) operating at an acceleration voltage of 100 kV was used to measure particle size and monitor aggregation state at different pH values, using carbon-coated copper grids. UV-Vis spectra were measured with an Agilent 8453 UV-Vis spectrophotometer. SERS spectra were acquired with a Renishaw InVia Reflex system. Two different laser lines (633 nm and 785 nm) were used for SERS excitation. ITC studies were carried out with a VP-ITC (MicroCal LLC, Northampton, MA), raw heat flow data were integrated using the software provided, and integrated heat data were subsequently analysed using IC ITC.[21,22] The pH of the solutions was measured using a PerpHect-Meter 370 pH meter equipped with a Thermo Scientific SEMI MICRO GLASS COMB pH electrode, or with a Hanna Instruments pH 210 pH meter equipped with a VWR 662-1759 glass electrode. An Applied Photophysics SX.18MV stopped-flow UV-Vis spectrophotometer was used to monitor the evolution of the assembly processes at pH values near and below the pK_a of PEN and NAP, as required.

Synthesis of gold and silver nanospheres

Gold sols were prepared by boiling aqueous $HAuCl_4$ (0.5 mM), in the presence of 1.5 mM sodium citrate, for 20 min.[23] For the synthesis of silver colloids ([Ag] = 0.1 mM) 0.01 M $AgClO_4$ was added to a cold aqueous solution of sodium citrate (0.3 mM) and sodium borohydride (1 mM) and allowed to react for 15 min.[24]

Assembly experiments

The nanoparticle assembly process was induced by adding different volumes of 1 M HCl solution to 2 mL of an Au@PEN or Au@NAP dispersion. The solution was homogenised by inversion and the kinetics of the assembly was recorded by UV-Vis spectroscopy. The solution was transferred into a cuvette and placed in the thermal static cell holder of the spectrophotometer. For the reversible assembly–disassembly experiments, 10 μL aliquots of 1 M HCl and NaOH solutions were alternately added to 2 mL of an Au@PEN or Au@NAP dispersion within a cuvette. After each addition and homogenisation by inversion the UV-Vis and SERS spectra at basic and acidic pH were recorded. One centimetre path length quartz cuvettes were used for all experiments.

Isothermal Titration Calorimetry (ITC)

ITC measurements were carried out in milli-Q water. Typically, a 0.25 or 0.5 mM solution of PEN or NAP solution was titrated into 1 mM (in terms of gold, corresponds to 9.1 nM nanoparticles) Au@citrate dispersion (but other combinations of concentrations gave similar results). Following baseline equilibration (typically three hours), successive injections (typically 3 to 4 μL) were performed at intervals of 1800 s. The instrument was operated in high-gain mode, applying a reference power of 10 μcal s^{-1} while stirring the sample cell contents at 239 rpm. Contrary to procedures typical for studies involving (bio)-macromolecular targets, solutions were not dialysed in order to maintain undisturbed naked Au nanoparticles prior to the titrations. Two different approaches for solution preparation were used. In the first one, the pH of the nanoparticle solution and the NAP or PEN solution was not adjusted (for these experiments, the NP solution typically had a pH in the range of 6–8 while PEN and NAP solutions typically had a pH near 4). In the second approach, titrations were carried out in the presence of 0.5 mM phosphate buffer, resulting in nearly matched cell and syringe solutions with pH near 7. Following a series of titrations involving gold nanoparticles, deterioration in baseline stability was typically observed, probably as a result of gold deposition in the sample cell. To remove deposited gold, the calorimeter sample cell was cleaned using a 5 mM aqueous sodium cyanide solution.[25] Briefly, the cell was filled with the cyanide solution, as usual, after which a "titration" was started, which resulted in effective stirring of the cell contents. This procedure was repeated twice after which the cell was further rinsed with water and ethanol, resulting in recovery of excellent baseline levels and stabilities.

Results and discussion

Surface modification with PEN and NAP

The surface modification of gold citrate with DL-penicillamine and *N*-acetyl-DL-penicillamine was studied through careful analysis of their mutual interaction by ITC measurements. In a typical experiment, a 0.25 or 0.5 mM solution of PEN or NAP was titrated into a 9–10 nM dispersion of gold nanoparticles at 25 °C and an initial pH between 6.3 and 7.0, *i.e.* above the pK_a of the system and therefore in the non-aggregating regime

This journal is © The Royal Society of Chemistry 2011

*J. Mater. Chem.*, 2011, **21**, 16880–16887 | 16881

(see below). Titrations were continued up to a final stoichiometry (PEN : NP or NAP : NP) that was significantly higher than the theoretical maximum surface coverage of the particles (*vide infra*) and the heat flow was recorded as usual (Fig. 1A for PEN; Fig. 1C for NAP). Each negative peak in the heat flow as a function of time corresponds to an injection, showing that binding is an exothermic process. Fig. 1A and C correspond to the raw calorimetric data obtained during titration and Fig. 1B and D are the plots of the integrated heat response obtained from the raw data plotted against the molar ratio (added amino acid : gold nanoparticle). Fig. 1B and D therefore correspond to binding isotherms of penicillamine and *N*-acetyl-penicillamine, respectively, on the gold surface allowing a first estimate of the number of molecules per gold nanoparticle for both thiols by visual inspection.

Fig. 1B and D clearly show typical transitions from a binding regime to a dilution regime around a stoichiometry of 2000 molecules per nanoparticle indicating the surface coverage of the nanoparticles. For most titrations, the heat effects following the transition are negligible. However, in some cases larger heat effects are observed following the transition which vary from titration to titration but are always smaller (less negative) than the heat effects prior to the transition. In principle, such heat effects could be indicative of a second binding event, but the fact that they are often absent and otherwise vary significantly between titrations suggest that they are not. In addition, titrations up to a molar ratio of at least 8000, *i.e.* three-fold the theoretical maximum surface coverage (*vide infra*), show no subsequent transitions. In the absence of a subsequent transition, the post-transition heat effects are assigned to dilution of the covered NPs, which even above the pK_a (*vide infra*) is likely to be different from the dilution of the naked NPs. In addition, the

variability in post-saturation heat effects is attributed to differences in pH adjustment (see Experimental) affecting the dilution heat effects of the excess PEN/NAP and the dilution heat effect of the fully covered nanoparticles (for examples, see Fig. S1 and S2†).

The multiple independent binding sites (MIS) model was selected as the simplest model satisfactorily reproducing typical titrations.[26] The fact that the MIS model reproduces data for NAP titrations well is remarkable in itself because it suggests that interactions between adjacent NAP molecules on the NP surface do not change significantly with increasing surface coverage. Titrations involving PEN, on the other hand, show a slight variation in heat effects before the main transition, suggesting some changes in the interactions between bound molecules of PEN as the surface density increases. Analysis of the integrated heat in terms of the MIS model provides the average number of PEN and NAP molecules per gold nanoparticle and further thermodynamic parameters (Table 1). The parameters listed in Table 1 are averages over at least eight experiments. The error margins are further confirmed by analysis of the simulated annealing trajectories (see Fig. S3A and S3B†, ESI). The binding parameters in buffered solution are essentially the same (see Table S1†), suggesting the absence of binding-linked (de) protonation[27] and the fact that our model selection is reasonable.

The binding equilibrium constants (K_a) and hence the Gibbs energy change for binding (ΔG) are similar for PEN and NAP. The enthalpy changes for binding (ΔH) are also very similar for PEN and NAP in water. With similar Gibbs energy changes and enthalpy changes, the entropy changes (ΔS) are obviously similar as well. Comparison with the ITC data reported by Rao *et al.*[20] for mercaptopropionic acid binding to gold nanorods shows that the shape of the enthalpogram is broadly the same. The observed
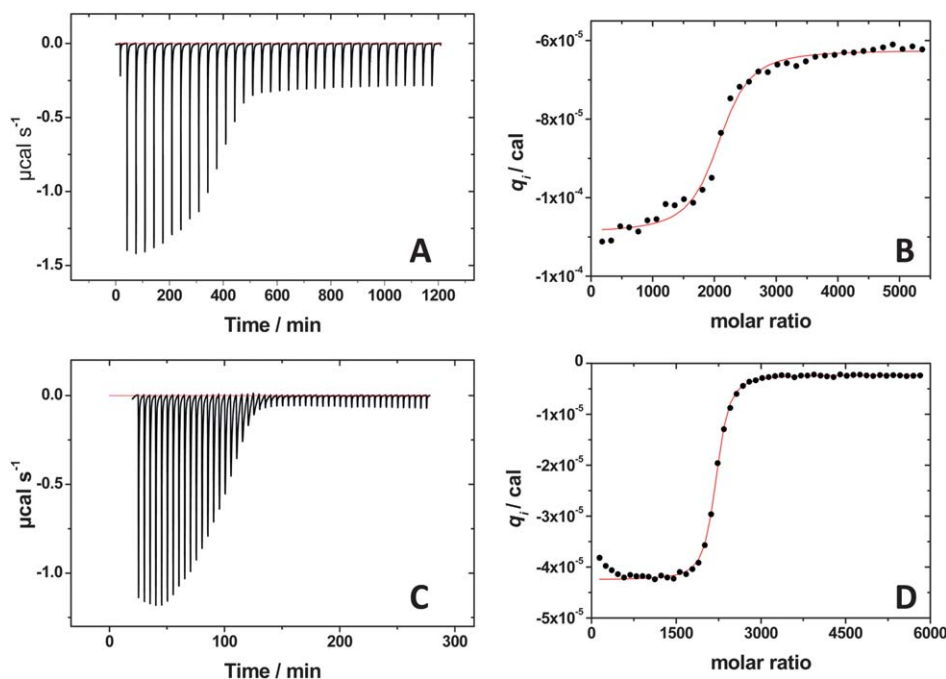
Fig. 1 Representative ITC data for PEN (A,B) and NAP (C,D) (0.5 mM in both cases) with Au nanoparticles (9.8 nM and 9.6 nM for PEN and NAP, respectively). Panels A and C show injection peaks (raw data *vs.* time), panels B and D show the integrated heat effects corresponding to the injection peaks (heat *vs.* AuNP/PEN,NAP molar ratio).

Table 1 Thermodynamic parameters for the interaction of PEN and NAP with gold nanoparticles at 25 °C[a]

	Stoichiometry	Degree of coverage	K_a/M^{-1}	ΔG/kcal mol^{-1}	ΔH/kcal mol^{-1}	ΔS/J K^{-1} mol^{-1}
PEN	$(2.0 \pm 0.5) \times 10^3$	40%	$(3.4 \pm 2.7) \times 10^7$	-9.9 ± 0.9	-25.8 ± 0.4	-53 ± 11
NAP	$(2.1 \pm 0.1) \times 10^3$	64%	$(2.1 \pm 0.5) \times 10^7$	-10.0 ± 0.2	-25.9 ± 0.1	-53 ± 2

[a] Error margins are standard deviations over at least 8 titrations.

stoichiometry is of the same order of magnitude, which is as much as one can expect considering the fact that very different nanoparticles were used. The enthalpy of interaction for the system reported by Rao *et al.* can be estimated from Fig. 4 in ref. 20 to be approximately -6 kcal mol^{-1}, considerably smaller than the value we find. We note, however, that Rao *et al.* used nanorods generated in the presence of CTAB and hence the nanoparticle surface properties prior to interaction with thiols are likely to be rather different.

Alternative data for comparison come from studies of interactions of thiols with macroscopic gold surfaces. For a 5′-thiolated duplex DNA, a binding equilibrium constant of $(1.5 \pm 1.3) \times 10^6$ M^{-1} was found.[28] Similarly, an estimate for the overall $\Delta G_{adsorption}$ of -5.5 kcal mol^{-1} has been suggested.[29] Finally, for adsorption of 1-octadecanethiol onto gold (in *n*-hexane), $\Delta G_{adsorption}$ was found to be temperature dependent and around -5.5 kcal mol^{-1}. A Van 't Hoff analysis provided ΔH_{ads} of -20 ± 1 kcal mol^{-1} and ΔS_{ads} of -48 ± 1 cal mol^{-1} K^{-1}.[30] These studies indicate equilibrium constants lower than those found here, but this may well be the result of the differences in solvents used and details of the state of the gold surface prior to addition of the thiol. The similarity between the enthalpy and entropy changes found for interactions with macroscopic gold surfaces and the values reported here is remarkable and strongly supports that our analysis yields reasonable results.
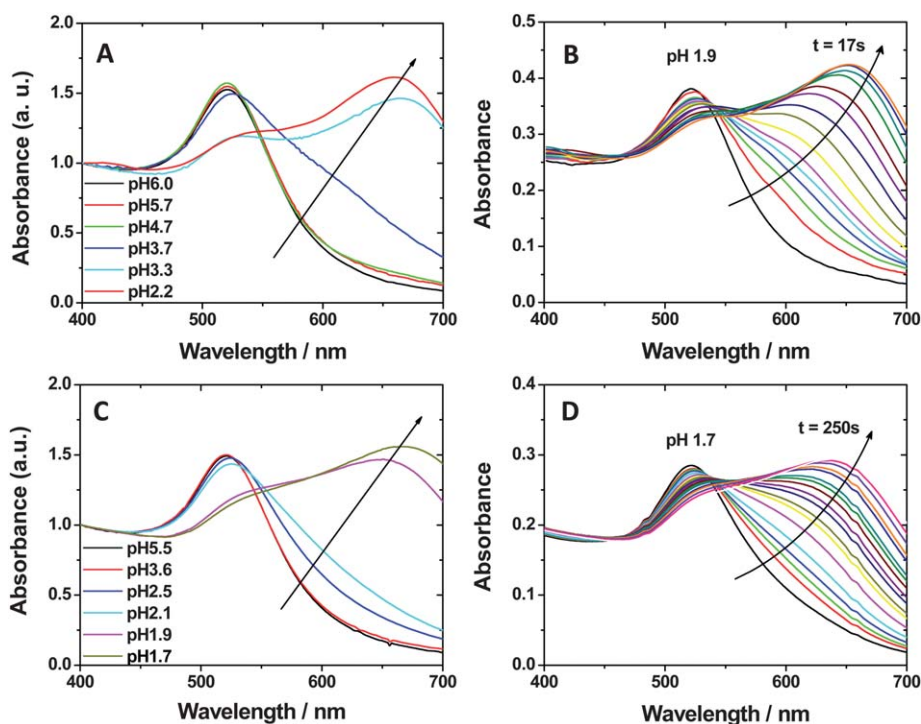
The degree of surface coverage is an important parameter that provides us with information about the surface packing and whether a monolayer or submonolayer of PEN/NAP is attached to the nanoparticle surface. The theoretical maximum number of PEN or NAP molecules attached to the nanoparticles was estimated considering as a first approximation each PEN/NAP molecule as an ellipsoid in contact with the nanoparticle surface, the ideal number of binding sites n_i per nanoparticle i is given by the ratio between the nanoparticle surface and the cross-section of a molecule considered as an ellipse (Fig. S4, ESI†). The average gold nanoparticle diameter was determined by TEM as 14.9 ± 1.8 nm (see Fig. S5, ESI†) and the surface areas occupied by the binding molecules (the cross-section area considering PEN and NAP as ellipsoids) are 0.142 nm^2 and 0.215 nm^2, for PEN and NAP, respectively (see Fig. S4, ESI†). Therefore, the theoretical stoichiometry for full surface coverage of a nanoparticle is 4978 and 3288 molecules for PEN and NAP, respectively. From these numbers, and the obtained stoichiometries from ITC, degrees of surface coverage of 40% and 64% were calculated for PEN and NAP, respectively, even though a surface coverage of 78.5% would be expected for a dense packing of ellipsoids in a monolayer. Clearly, in both cases the surface coverage should be considered as a submonolayer. Interestingly, PEN shows a lower degree of packing compared to NAP (40% *vs.* 64%), which may be related to the charge difference between them.

pH dependent assembly

The penicillamine modified metal nanoparticles show pH dependent optical response. Fig. 2A and C show the spectra of gold nanoparticle dispersions modified with the stoichiometric amount of PEN and NAP at different pH, as indicated. It can be observed that the nanoparticle dispersions are stable over a wide pH range (pH > 4) but when the pH is decreased to 3.7 (for PEN) and 2.6 (for NAP), the localized surface plasmon resonance (LSPR) band is observed to broaden and red-shift. Further decrease in the solution pH leads to evolution of a new band located around 650 nm. At pH values of 3.3 for PEN and 1.9 for NAP, the red-shift of this new band is maximum, meaning that for lower pH similar spectra are recorded although the final equilibrium spectrum is reached faster. As an example, Fig. 2B and D (and Fig. S6 in ESI†) show the time evolution of the optical spectra of gold nanoparticle dispersions stabilized by PEN and NAP, respectively, at low pH. Interestingly, gold nanoparticles stabilized by PEN seem to reach equilibrium faster than those stabilized with NAP. Similar results were obtained when other acid sources were employed such as sulfuric acid or nitric acid (see Fig. S7, ESI†). Control experiments at similar pH values were conducted with citrate stabilized gold nanoparticles, to confirm the crucial role played by the PEN/NAP surface modification. A pH independent behaviour was found in this case, which indicates that the particles remain fully stable in a wide pH range (see Fig. S8, ESI†).

TEM analysis of the samples (see Fig. 3A and experimental details for sample preparation) confirmed that at neutral and basic pH the particles are well dispersed and randomly distributed on the TEM grid, while at acidic pH the particles tend to coalesce, in agreement with the observed pH-dependent optical response. As the pH of the solution decreases the particles tend to aggregate, leading to plasmon coupling, which results in broadening and red-shift of the LSPR bands.[31] Because the extent of electronic interactions and plasmon coupling depends on factors such as particle size,[32] interparticle distance,[33] number of particles in the aggregate,[34] or shape of the aggregates, the precise shape of the new bands may vary from sample to sample.

To understand the origin of nanoparticle aggregation in this system, we need to consider the nature of the thiol containing amino acids. DL-Penicillamine contains carboxylic acid, amine and thiol groups with pK_a values of 1.8, 10.5 and 7.9, respectively.[35] Based on the well-established Au–sulfur chemistry, we propose that PEN and NAP are immobilized on the gold surface *via* the thiol group. Therefore, the stability of the PEN/NAP modified particles at different pH will be determined by the subtle protonation balance between carboxylic and amine groups. It should be pointed out that it has been reported that the pK_a values of the carboxylic groups might be affected by the

This journal is © The Royal Society of Chemistry 2011

J. Mater. Chem., 2011, **21**, 16880–16887 | 16883

Fig. 2 (A) and (C) are UV-Vis spectra of gold nanoparticle dispersions stabilized with PEN and NAP, respectively, at different pH values. (B) and (D) show the time evolution of the UV-Vis spectra during aggregation at low pH (as indicated in the labels) for PEN and NAP, respectively.

binding to metal nanoparticles, being shifted to slightly higher values.[36,37] We have experimentally observed that aggregation starts to take place at pH 3.7 for PEN and 2.5 for NAP, where the amine groups are protonated while the carboxylic groups may start to be protonated. Two different mechanisms have been

proposed to explain nanoparticle assembly driven by amine and carboxylic acid functionalities: (a) the assembly *via* electrostatic interactions between zwitterionic amino acids has been proposed for gold nanospheres[38] and nanorods[39] (Scheme 1A); (b) the assembly by hydrogen bonding was recently reported for
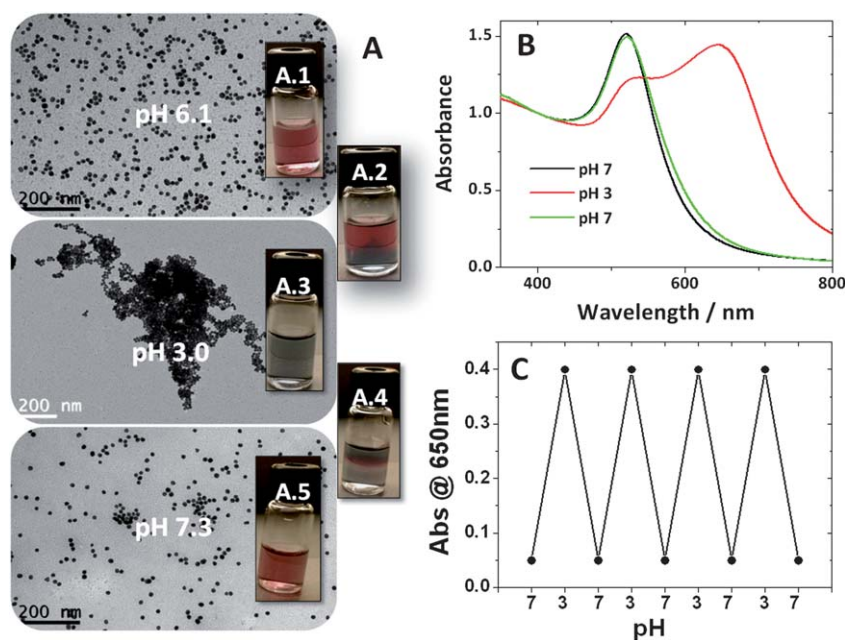
Fig. 3 (A) Representative TEM images of gold nanoparticles and photographs of their corresponding dispersions, at different pH as indicated in the labels. (B) Variation of UV-Vis spectra of an Au–PEN dispersion upon successive decrease and increase of pH, as indicated in the labels. (C) Variation of the absorbance at 650 nm when the pH was cycled between 7 and 3. In all cases [Au] = 0.1 mM and the amount of PEN added corresponded to a submonolayer, as determined by ITC.

16884 | *J. Mater. Chem.*, 2011, **21**, 16880–16887

This journal is © The Royal Society of Chemistry 2011

glutathione assembly of gold nanospheres and mercaptophenol assembly of gold nanorods (Scheme 1B).[40,41]

Under our experimental conditions, at pH between 7 and 4 the amine should be protonated while the carboxylic acid remains deprotonated, no aggregation being observed. Therefore, assembly *via* electrostatic interaction of zwitterionic groups (Scheme 1A) can be neglected. Consequently, the pH dependent extension of the nanoparticles assembly should be driven by the development of a stronger hydrogen-bonding character as the acid groups become protonated (Scheme 1B). The assembly is therefore driven by the pK_a of the acid functionality and therefore the pH of the solution. However, the specific nature of the molecule also seems to play an important role since the aggregation rate was found to be significantly higher for PEN than for NAP. Fig. 2B and D show the spectral evolution during Au aggregation for PEN and NAP at pH well below their respective pK_a values. In this respect, the steric hindrance of the substituted amine for NAP might be responsible for a lower assembly rate as compared to PEN.

Reversible assembly

The hydrogen bonding origin of the nanoparticle assembly, together with the high stability of the particles upon modification with the thiol-containing amino acids, allows the reversible assembly and disassembly of the nanoparticles through changes in solution pH. The reversible assembly was characterized by TEM, UV-Vis and SERS spectroscopies. Fig. 3A shows representative TEM images and photographs of the same sample at different pH for a dispersion of PEN-stabilized gold nanoparticles. At pH 6.1 the red colour characteristic of the 15 nm gold nanoparticles is observed (Fig. 3A.1), corresponding to separate particles that are homogeneously distributed on the TEM grid. Upon addition of hydrochloric acid, the blue colour at the bottom part of the solution indicates that particle aggregation starts there, due to the higher density of the acid solution (Fig. 3A.2). Obviously, after homogenisation by inversion, the bluish colour is extended to the whole solution (Fig. 3A.3). At pH = 3, the TEM images show clustering of the particles on the grid. However, increasing again the solution pH by addition of sodium hydroxide shows recovery of the initial red colour, demonstrating the fully reversible assembly and disassembly process. Similar results were obtained for NAP stabilized particles (data not shown).

The extent of reversibility in this process can be observed by naked-eye but more precisely by recording the UV-Vis spectra at alternating pH values. Fig. 3B clearly shows fully reversible changes in the absorption at 650 nm for the same solution during alternating pH variation between 7 and 3. For these particular conditions, reversibility has been confirmed up to the 15th cycle.
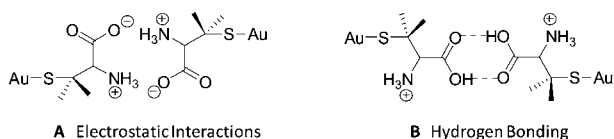
After so many cycles of acid and base additions, the ionic strength of the solution is high, leading to a decrease of the screening length and consequently to irreversible aggregation of the particles.

Although all the results that we have shown so far were obtained with gold nanoparticles, completely similar behaviour was observed for citrate stabilized silver nanoparticles.[42] After surface functionalization with PEN, aggregation can be induced at pH 3, leading to a decrease of the characteristic silver LSPR band located at 400 nm and appearance of a broad shoulder around 500 nm. Again, switching the pH to values between neutral and slightly basic values leads to complete disaggregation of the particles (see Fig. S9, ESI†).
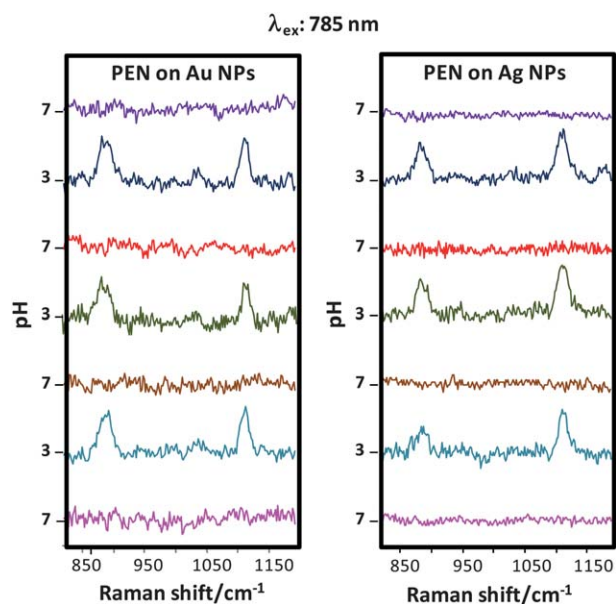
SERS characterization

The ability of metallic nanostructures to enhance the Raman signal is particularly efficient when the probe molecules are located at small gaps between nanoparticles, since the electromagnetic field is particularly high at such "hot spots".[43] Thus, SERS provides us with a sensitive tool to carry out additional characterization of the reversibility of the pH dependent assembly. SERS measurements were carried out on gold and silver nanoparticles capped with either PEN or NAP. Fig. 4 shows Raman and SERS spectra of PEN acquired using two laser lines, 633 and 785 nm. The SERS spectra recorded upon excitation with both laser lines fit band to band and are dominated by 545 and 578 cm^{-1} (CS stretching), 888 cm^{-1} (CH_3 rocking) and 1117 cm^{-1} (CC stretching and CN stretching) in good agreement with previously reported values.[44] Furthermore, from comparison of Raman and SERS spectra for PEN, with 633 nm excitation, we find that the band at 2570 cm^{-1}, ascribed to SH stretching, is present in the Raman but not in the SERS spectrum, indicating that the binding of the amino acid to the particles surface does indeed take place through the thiol functional group. It should be pointed out that the SERS spectrum was recorded at pH 3, therefore the absence of the SH stretching band cannot be ascribed to the deprotonated thiol.[44]

Interestingly, we found that the pH of the solution has a large influence on the SERS signal of PEN. As a representative example, Fig. 5 shows the SERS spectra of PEN on gold and
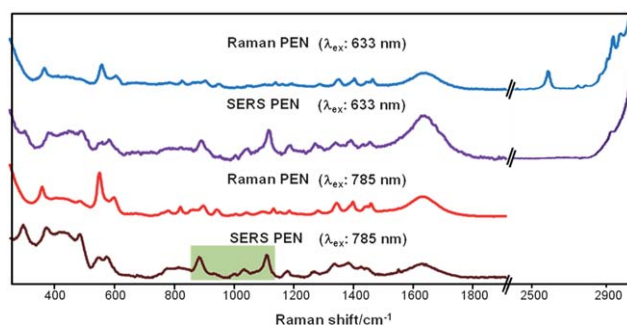
Fig. 4 Raman and SERS spectra of PEN (at pH 3) when excited with a visible laser line (633 nm) and an infrared laser line (785 nm). The characteristic band of S–H stretching (2570 cm^{-1}) completely disappears in SERS as a consequence of the S covalent bonding to metal at the nanoparticles surface.

Scheme 1 Illustration of PEN-induced assembly models, when driven by either electrostatic (A) or hydrogen bonding (B) interactions.

A Electrostatic Interactions

B Hydrogen Bonding

Fig. 5 SERS spectra of Au–PEN (left) and Ag–PEN (right) when excited with a 785 nm laser line, at alternating pH values.

silver colloids at pH 7 and pH 3. It can be observed that no vibrational pattern could be recorded at pH 7, when the gold/silver nanoparticles are colloidally stable and thus far away from each other. However, at pH 3, when the particles are aggregated, a well-defined SERS spectrum was consistently obtained. This undoubtedly reflects the formation of hot spots when the particles get close to each other. Because the PEN molecules serve as anchoring points, they must be located at the interstitial gaps between metal nanoparticles, precisely where hot spots are created. Further evidence of the dynamic nature of such hot spot formation was obtained by cycling the solution pH between 7 and 3, which resulted in recording of the SERS signal only when the particles are in the aggregated form (pH 3). Similar results were obtained for NAP-capped Au and Ag (not shown).

Conclusions

Isothermal titration calorimetry (ITC) has proven a powerful technique to evaluate and quantify the surface coverage of thiol-capped gold nanoparticles obtained through ligand exchange in aqueous solution. ITC evaluation of the adsorption of PEN and NAP on citrate-stabilized gold nanoparticles yields values of 40% and 64% for the degree of surface coverage, respectively, corresponding to well below full monolayer coverage. Hydrogen bonding between amino acids adsorbed on different nano-particles appears to be responsible for the reversible assembly of gold/silver nanoparticles upon pH changes. Finally, the pH-controlled reversible assembly of gold and silver nanoparticles mediated by PEN or NAP leads to strong LSPR coupling, resulting in huge local enhancement of the electric field, *i.e.* hot-spot formation. The reversible formation of hot-spots was demonstrated through comparison of the SERS spectra between aggregated and stable colloids, upon cyclic pH changes. This study is expected to serve as a reference for the design of nano-particle assembly methods based on hydrogen bonding,

including detailed characterization of surface coverage with capping molecules.

References

1 M. Grzelczak, J. Vermant, E. M. Furst and L. M. Liz-Marzán, *ACS Nano*, 2010, **4**, 3591–3605.
2 K. J. M. Bishop, C. E. Wilmer, S. Soh and B. A. Grzybowski, *Small*, 2009, **5**, 1600–1630.
3 S. Liu and Z. Tang, *J. Mater. Chem.*, 2010, **20**, 24–35.
4 D. Fava, M. A. Winnik and E. Kumacheva, *Chem. Commun.*, 2009, 2571–2573.
5 M. Fialkowski, K. J. M. Bishop, R. Klajn, S. K. Smoukov, C. J. Campbell and B. A. Grzybowski, *J. Phys. Chem. B*, 2006, **110**, 2482–2496.
6 Z. Sun, W. Ni, Z. Yang, X. Kou, L. Li and J. Wang, *Small*, 2008, **4**, 1287–1292.
7 S. Si, M. Raula, T. K. Paira and T. K. Mandal, *ChemPhysChem*, 2008, **9**, 1578–1584.
8 I. Lagzi, B. Kowalczyk, D. Wang and B. A. Grzybowski, *Angew. Chem., Int. Ed.*, 2010, **49**, 8616–8619.
9 (*a*) A. Sánchez-Iglesias, M. Grzelczak, J. Pérez-Juste and L. M. Liz-Marzán, *Angew. Chem., Int. Ed.*, 2010, **49**, 9985–9989; (*b*) Z. Zhu, H. Meng, W. Liu, X. Liu, J. Gong, X. Qiu, L. Jiang, D. Wang and Z. Tang, *Angew. Chem., Int. Ed.*, 2011, **50**, 1593–1596.
10 L. Maus, J. P. Spatz and R. Fiammengo, *Langmuir*, 2009, **25**, 7910–7917.
11 L. Maus, O. Dick, H. Bading, J. P. Spatz and R. Fiammengo, *ACS Nano*, 2010, **4**, 6617–6628.
12 *Biocalorimetry 2: Applications of Calorimetry in the Biological Sciences*, ed. J. E. Ladbury and ML. Doyle, 2004.
13 G. Thompson, D. Owen, P. A. Chalk and P. N. Lowe, *Biochemistry*, 1998, **37**, 7885–7891.
14 A. Kunne, M. Sieber, D. Meierhans and R. K. Allemann, *Biochemistry*, 1998, **37**, 4217–4223.
15 M. R. Wenk and J. Seelig, *Biochemistry*, 1998, **37**, 3909–3916.
16 M. De, C.-C. You, S. Srivastava and V. M. Rotello, *J. Am. Chem. Soc.*, 2007, **129**, 10747–10753.
17 S. Lindman, I. Lynch, E. Thulin, H. Nilsson, K. A. Dawson and S. Linse, *Nano Lett.*, 2007, **7**, 914–920.
18 A. Gourishankar, S. Shukla, K. N. Ganesh and M. Sastry, *J. Am. Chem. Soc.*, 2004, **126**, 13186–13187.
19 H. Joshi, P. S. Shirude, V. Bansal, K. N. Ganesh and M. Sastry, *J. Phys. Chem. B*, 2004, **108**, 11535–11540.
20 N. Varghese, S. R. C. Vivekchand, A. Govindaraj and C. N. R. Rao, *Chem. Phys. Lett.*, 2008, **450**, 340–344.
21 N. J. Buurma and I. Haq, *J. Mol. Biol.*, 2008, **381**, 607–621.
22 N. J. Buurma and I. Haq, *Methods*, 2007, **42**, 162–172.
23 B. V. Enüstün and J. Turkevich, *J. Am. Chem. Soc.*, 1963, **85**, 3317–3328.
24 T. Ung, L. M. Liz-Marzán and P. Mulvaney, *Langmuir*, 1998, **14**, 3740–3748.
25 Based on the EPA report "Toxicological Review of Hydrogen Cyanide and Cyanide Salts" (EPA/635/R-08/016F), we prepared only 50 mL of a stock solution of 5 mM sodium cyanide for safety reasons. The use of only 2.5 mL of this solution when cleaning the calorimeter cell further reduces risk. We stress, however, that others must make their own individual assessment based on the available literature. We further stress that for the preparation of the stock solution itself, all the usual safety measures for handling cyanides need to be observed. All cyanide solutions were destroyed using bleach after use.

26 We note that analysis in terms of a single type of binding sites includes the assumption that the post-transition heat effects are indeed caused by dilution heat effects only. If the latter is incorrect, then both binding constants and interaction enthalpies are lower estimates. The stoichiometry of the interaction, however, is not sensitive to this assumption.

27 B. M. Baker and K. P. Murphy, *Biophys. J.*, 1996, **71**, 2049–2055.

28 M. Yang, H. C. M. Yau and H. L. Chan, *Langmuir*, 1998, **14**, 6121–6129.

29 J. B. Schlenoff, M. Li and H. Ly, *J. Am. Chem. Soc.*, 1995, **117**, 12528–12536.

30 H. M. Schessler, D. S. Karpovich and G. J. Blanchard, *J. Am. Chem. Soc.*, 1996, **118**, 9645–9651.

31 T. Ung, L. M. Liz-Marzán and P. Mulvaney, *J. Phys. Chem. B*, 2001, **105**, 3441–3452.

32 S. Vial, I. Pastoriza-Santos, J. Pérez-Juste and L. M. Liz-Marzán, *Langmuir*, 2007, **23**, 4606–4611.

33 P. K. Jain, W. Huang and M. A. El-Sayed, *Nano Lett.*, 2007, **7**, 2080–2088.

34 Z. Sun, W. Ni, Z. Yang, X. Kou, L. Li and J. Wang, *Small*, 2008, **4**, 1287–1292.

35 A. E. Martell and R. M. Smith, *Critical Stability Constants, 1*, Plenum Press, NewYork, 1989, vol. 6, 2nd suppl., p. 21.

36 (*a*) W. X. Zheng, M. M. Maye, F. L. Leibowitz and C. J. Zhong, *Analyst*, 2000, **125**, 17–20; (*b*) W. X. Zheng, M. M. Maye, F. L. Leibowitz and C. J. Zhong, *Anal. Chem.*, 2000, **72**, 2190–2199; (*c*) J. Luo, N. Kariuki, L. Han, M. M. Maye, L. W. Moussa, S. R. Kowaleski, S. R. Kirk, M. Hepel and C. J. Zhong, *J. Phys. Chem. B*, 2002, **106**, 9313–9321.

37 D. Wang, R. J. Nap, I. Lagzi, B. Kowalczyk, S. Han, B. A. Grzybowski and I. Szleifer, *J. Am. Chem. Soc.*, 2011, **133**, 2192–2197.

38 S. Zhang, X. Kou, Z. Yang, Q. Shi and G. D. Stucky, *Chem. Commun.*, 2007, 1816–1818.

39 P. K. Sudeep, S. T. S. Joseph and K. G. Thomas, *J. Am. Chem. Soc.*, 2005, **127**, 6516–6517.

40 I.-I. S. Lim, D. Mott, W. Ip, P. N. Njoki, Y. Pan, S. Zhou and C.-J. Zhong, *Langmuir*, 2008, **24**, 8857–8863.

41 W. Ni, R. A. Mosquera, J. Pérez-Juste and L. M. Liz-Marzán, *J. Phys. Chem. Lett.*, 2010, **1**, 1181–1185.

42 In the case of the citrate stabilized silver nanoparticle no attempt to characterize the stochiometry by ITC was performed due to the low monodispersity of the samples, which makes the estimation of the surface area unreliable.

43 L. Brus, *Acc. Chem. Res.*, 2008, **41**, 1742–1749.

44 M. R. López-Ramírez, J. F. Arenas, J. C. Otero and J. L. Castro, *J. Raman Spectrosc.*, 2004, **35**, 390–394.

This journal is © The Royal Society of Chemistry 2011

J. Mater. Chem., 2011, **21**, 16880–16887 | 16887